

See discussions, stats, and author profiles for this publication at: <https://www.researchgate.net/publication/5796173>

# Inhibitors Bound to Ca<sup>2+</sup> -Free Sarcoplasmic Reticulum Ca<sup>2+</sup> -ATPase Lock Its Transmembrane Region but Not Necessarily Its Cytosolic Region, Revealing the Flexibility of the Loops...

ARTICLE in BIOCHEMISTRY · JANUARY 2008

Impact Factor: 3.02 · DOI: 10.1021/bi701855r · Source: PubMed

CITATIONS

10

READS

183

6 AUTHORS, INCLUDING:



**Cédric Montigny**

French National Centre for Scientific Research

35 PUBLICATIONS 384 CITATIONS

SEE PROFILE



**Martin Picard**

French National Centre for Scientific Research

36 PUBLICATIONS 620 CITATIONS

SEE PROFILE



**Guillaume Lenoir**

Atomic Energy and Alternative Energies Com...

22 PUBLICATIONS 514 CITATIONS

SEE PROFILE



**Philippe Champeil**

French Institute of Health and Medical Resea...

114 PUBLICATIONS 3,470 CITATIONS

SEE PROFILE

# Inhibitors Bound to $\text{Ca}^{2+}$ -Free Sarcoplasmic Reticulum $\text{Ca}^{2+}$ –ATPase Lock Its Transmembrane Region but Not Necessarily Its Cytosolic Region, Revealing the Flexibility of the Loops Connecting Transmembrane and Cytosolic Domains<sup>†</sup>

Cédric Montigny,<sup>‡,§</sup> Martin Picard,<sup>‡,§,||</sup> Guillaume Lenoir,<sup>‡,§,⊥</sup> Carole Gauron,<sup>‡,§</sup> Chikashi Toyoshima,<sup>▽</sup> and Philippe Champeil<sup>\*,‡,§</sup>

CNRS, URA 2096 (Protéines Membranaires Transductrices d'Énergie), F-91191 Gif-sur-Yvette, France, CEA, iBiTecS (Institut de Biologie et Technologies de Saclay), F-91191 Gif-sur-Yvette, France, and Institute of Molecular and Cellular Biosciences, University of Tokyo, Bunkyo-ku, Tokyo 113-0032, Japan

Received September 11, 2007; Revised Manuscript Received October 16, 2007

**ABSTRACT:**  $\text{Ca}^{2+}$ -free crystals of sarcoplasmic reticulum  $\text{Ca}^{2+}$ –ATPase have, up until now, been obtained in the presence of inhibitors such as thapsigargin (TG), bound to the transmembrane region of this protein. Here, we examined the consequences of such binding for the protein. We found that, after TG binding, an active site ligand such as beryllium fluoride can still bind to the ATPase and change the conformation or dynamics of the cytosolic domains (as revealed by the protection afforded against proteolysis), but it becomes unable to induce any change in the transmembrane domain (as revealed by the intrinsic fluorescence of the membranous tryptophan residues). TG also obliterates the Trp fluorescence changes normally induced by binding of MgATP or metal-free ATP, as well as those induced by binding of  $\text{Mg}^{2+}$  alone. In the nucleotide binding domain, the environment of Lys<sup>515</sup> (as revealed by fluorescein isothiocyanate fluorescence after specific labeling of this residue) is significantly different in the ATPase complex with aluminum fluoride and in the ATPase complex with beryllium fluoride, and in the latter case it is modified by TG. All these facts document the flexibility of the loops connecting the transmembrane and cytosolic domains in the ATPase. In the absence of active site ligands, TG protects the ATPase from cleavage by proteinase K at Thr<sup>242</sup>–Glu<sup>243</sup>, suggesting TG-induced reduction in the mobility of these loops. 2,5-Di-*tert*-butyl-1,4-dihydroxybenzene or cyclopiazonic acid, inhibitors which also bind in or near the transmembrane region, also produce similar overall effects on  $\text{Ca}^{2+}$ -free ATPase.

Sarcoplasmic reticulum (SR)<sup>1</sup>  $\text{Ca}^{2+}$ –ATPase (SERCA1a) is an ion pump belonging to the family of P-type ATPases, responsible in muscle cells for active transport of  $\text{Ca}^{2+}$  from the cytosol into the sarcoplasmic reticulum lumen (see, e.g., refs 1–6 for review): the resulting reduction of the cytosolic free  $\text{Ca}^{2+}$  concentration triggers muscle relaxation. This

active transport requires ATP hydrolysis as the energy source, and its catalytic cycle has been studied at length. At some step during ATP hydrolysis, the pump's affinity for  $\text{Ca}^{2+}$  changes from high to low, coupled with topological reorientation of the binding sites from one side of the membrane to the other (with intermediate “occluded” species). The catalytic cycle comprises transitions between various intermediates, some of which are phosphorylated (hence the name of the “P-type” family) at a critical aspartate residue in the catalytic site (e.g., the so-called  $\text{Ca}_2\cdot\text{E1P}$  or  $\text{E2P}$  forms). In 2000, the detergent-solubilized purified ATPase was crystallized in the presence of  $\text{Ca}^{2+}$ , and in subsequent years other forms of the ATPase, thought to be fair analogues of various catalytic intermediates, were also obtained, allowing elucidation of the main structural features required for ATP-driven ion pumping (7–18).

However, the traditional question of the extent to which crystalline structures reflect the more dynamic structures of an enzyme during its catalytic cycle can of course be raised (see, e.g., refs 19 and 20). This is especially the case for the structures obtained in the absence of  $\text{Ca}^{2+}$ , as the crystals corresponding to these forms have been obtained, until now, by compensating the instability of detergent-solubilized ATPase in the absence of  $\text{Ca}^{2+}$  (see, e.g., refs 21–24) by the addition of inhibitors (such as those mentioned in refs

<sup>†</sup> We thank the Human Frontier Science Program Organization for support, Grant RGP 0060/2001-M.

\* To whom correspondence should be addressed. Phone: 33-1-6908-3731. Fax: 33-1-6908-8139. E-mail: philippe.champeil@cea.fr.

<sup>‡</sup> CNRS.

<sup>§</sup> CEA.

<sup>||</sup> Present address: Laboratoire de Cristallographie & RMN Biologiques, CNRS UMR 8015 and Université Paris Descartes, 4 avenue de l'Observatoire, 75270 Paris Cedex 06, France.

<sup>⊥</sup> Present address: Department of Membrane Enzymology, Bijvoet Center and Institute of Biomembranes, Utrecht University, Padualaan 8, 3584 CH Utrecht, The Netherlands.

<sup>▽</sup> University of Tokyo.

<sup>1</sup> Abbreviations: SR, sarcoplasmic reticulum; ATPase, adenosine triphosphatase; E2 and E1, nonphosphorylated forms of  $\text{Ca}^{2+}$ –ATPase; E2P and E1P, phosphorylated forms of  $\text{Ca}^{2+}$ –ATPase, respectively ADP-insensitive or ADP-sensitive; TG, thapsigargin; BHQ, 2,5-di-*tert*-butyl-1,4-dihydroxybenzene; CPA, cyclopiazonic acid; prK, proteinase K; SDS–PAGE, sodium dodecyl sulfate–polyacrylamide gel electrophoresis; EGTA, [ethylenbis(oxyethylenitrilo)]tetraacetic acid; Mops, 4-morpholinepropanesulfonic acid; Tris, tris(hydroxymethyl)aminomethane; Mes, 4-morpholineethanesulfonic acid; FITC, fluorescein 5-isothiocyanate.

25–27). Note that crystals of a given form of  $\text{Ca}^{2+}$ -free ATPase obtained in the presence of different inhibitors (thought to act on the protein similarly) reveal slightly different structures (15–17). In a previous work, we have shown that adding inhibitors such as thapsigargin (TG), 2,5-di-*tert*-butyl-1,4-dihydroxybenzene (BHQ), or cyclopiazonic acid (CPA) to  $\text{Ca}^{2+}$ -free ATPase complexed with  $\text{BeF}_x$  (a transition-state analogue of “E2P”) indeed prevents the ATPase  $\text{Ca}^{2+}$  binding pocket from opening toward the lumen, in contrast with what is considered to happen with the “normal” E2P form, and with the unfortunate consequence that, in the presence of such inhibitors, we may never be able to obtain crystals showing the ATPase structure with an *open*  $\text{Ca}^{2+}$  release pathway from the transport sites toward the lumen (28).

In the present work, we further document the effects of TG, BHQ, and CPA on  $\text{Ca}^{2+}$ -free ATPase. By monitoring the fluorescence changes occurring either in one of the cytosolic domains or within the transmembrane domain (thanks to a fluorescein label attached to  $\text{Lys}^{515}$  in the nucleotide binding domain or to the ATPase intrinsic tryptophan residues, respectively) upon addition of specific ligands such as fluoride, vanadate,  $\text{Mg}^{2+}$ , or ATP, we now show that the presence of TG or related inhibitors *fixes* the structure of the ATPase *transmembrane domain* and prevents it from experiencing the changes which would normally have occurred in the absence of the inhibitor, *without necessarily* preventing binding events in the cytosolic domains from occurring. This is presumably a consequence of the likely *flexibility* of the loops connecting the A-domain and the transmembrane part of the ATPase and probably explains why the various structures previously described for crystalline  $\text{Ca}^{2+}$ -free ATPase forms have all been found to be very similar in their transmembrane domains, irrespective of the bound ligands and conformations in their cytosolic domains. By monitoring the proteolytic susceptibility of a loop intervening between the ATPase transmembrane and cytosolic domains, we also document the effect of the inhibitors on the protein average structure or dynamics.

## EXPERIMENTAL PROCEDURES

**Chemicals.** TG (the stock solution was 1 mg/mL in DMSO, i.e., about 1.5 mM) was from VWR International (no. 586005, Fontenay-sous-bois, France), BHQ (the stock solution was 22 mg/mL in DMSO, i.e., 100 mM) was from Aldrich (no. 11,297-6, Saint Quentin Fallavier, France), and CPA (the stock solution was 10 mg/mL in DMSO, i.e., about 30 mM) was from Sigma (no. C1530, Saint Quentin Fallavier, France). Proteinase K (the stock solutions were 6 or 1.5 mg/mL in 10 mM Tris–Cl, pH 7.4) was from Roche Diagnostics (no. 745723, Meylan, France).

**Proteolysis by Proteinase K.** For controlled proteolysis, SR membrane vesicles (prepared as in refs 28 and 29) were treated with proteinase K (prK) under conditions described in the corresponding figure captions. As previously (30, 31), proteolysis was stopped by adding 0.5–1 mM PMSF to the samples and transferring them on ice for at least 10 min. After proteolysis arrest, the samples were diluted 10-fold into a 4 M urea-containing denaturation buffer (otherwise as described in ref 32) and boiled for 60 s, and aliquots were loaded onto an SDS–PAGE Laemmli gel (33) prepared in

the presence of 1 mM  $\text{Ca}^{2+}$  (8–12% acrylamide, as needed). Depending on the experiment and on the desired level of response linearity, 4 or 2  $\mu\text{g}$  of protein was loaded per lane; after Coomassie Blue staining, the intensity of the individual peptide bands was deduced from gel scanning. The electrophoresis miniprotein 2 supply, the GS700 densitometer, and Molecular Analyst and Quantity One software were provided by Bio-Rad SA (Marnes-la-Coquette, France); low molecular weight (LMW) markers were from GE Healthcare (Vélizy, France).

**Fluorescence Measurements.** Fluorescence measurements were carried out with a SPEX Fluorolog spectrofluorometer provided by Horiba/Jobin-Yvon (Longjumeau, France). The intrinsic fluorescence of the ATPase was recorded with excitation and emission wavelengths set at 290 nm (or 298 nm; see the figure captions) and 330 nm (or 320 nm), respectively (bandwidths were 2 and 10 nm, respectively), with SR membranes at 0.1 mg/mL protein in a thermostated and continuously stirred cuvette (see, e.g., ref 19). Extrinsic fluorescence of FITC-labeled SR membranes (suspended at 0.02 mg/mL protein) was also recorded (ATPase labeling with FITC had been performed as described (34), except that FITC had been initially diluted in dimethyl sulfoxide (DMSO) instead of dimethylformamide); excitation and emission wavelengths were then set at 495 and 520 nm (bandwidths were 2 and 10 nm, respectively).

**Filtration Measurements.** SR membranes were first suspended at 0.1 mg/mL protein, with or without inhibitors (TG at 1  $\mu\text{g}/\text{mL}$  (about 1.5  $\mu\text{M}$ ), CPA at 0.3  $\mu\text{g}/\text{mL}$  (about 1.35  $\mu\text{M}$ ), or BHQ at 30  $\mu\text{M}$ ), in a  $\text{Ca}^{2+}$ -free buffer in the presence or absence of  $\text{Mg}^{2+}$  at pH 7 and 20 °C (see the figure captions). Then, at time zero, 30  $\mu\text{M}$  [ $\gamma$ - $^{32}\text{P}$ ]ATP together with 300  $\mu\text{M}$  [ $^3\text{H}$ ]glucose was added from a concentrated solution (already containing the two isotopes). After various periods, aliquots (2.5 mL, i.e., about 0.25 mg of protein) were loaded onto two HA filters (Millipore, no. HAWP02500, Saint Quentin en Yvelines, France) on top of each other, under vacuum. The two filters, without rinsing, were counted individually in a scintillation counter, with [ $^3\text{H}$ ]glucose in each filter serving as a marker of the background unbound ATP (trapped in this filter together with the wetting volume). In the upper filter, unbound ATP was subtracted from the total ATP, to give the amount of ATP bound specifically to the ATPase. The lower filter served to check that SR membranes were adsorbed onto the upper filter only (see, e.g., ref 28 or 34 for related filtration experiments).

## RESULTS

**Effects of TG or Other Inhibitors on “E2P-Related” Forms of  $\text{Ca}^{2+}$ -Free ATPase: Proteolysis and Intrinsic Fluorescence Experiments.** In a remarkable series of papers, Danko and colleagues previously demonstrated that  $\text{Ca}^{2+}$ -free ATPase becomes fully resistant to proteolysis by proteinase K after formation of E2P-related species from either orthovanadate or fluoride complexes (or, to some extent, from phosphate itself) (35, 36). These authors also mentioned that protection by such phosphate analogues was still observed in the presence of TG. As a preliminary check, we repeated those experiments under our own favorite conditions (Supplemental Figure S3 in ref 28) for forming E2P-like species, i.e., at pH 7 in the presence of KCl and the additional

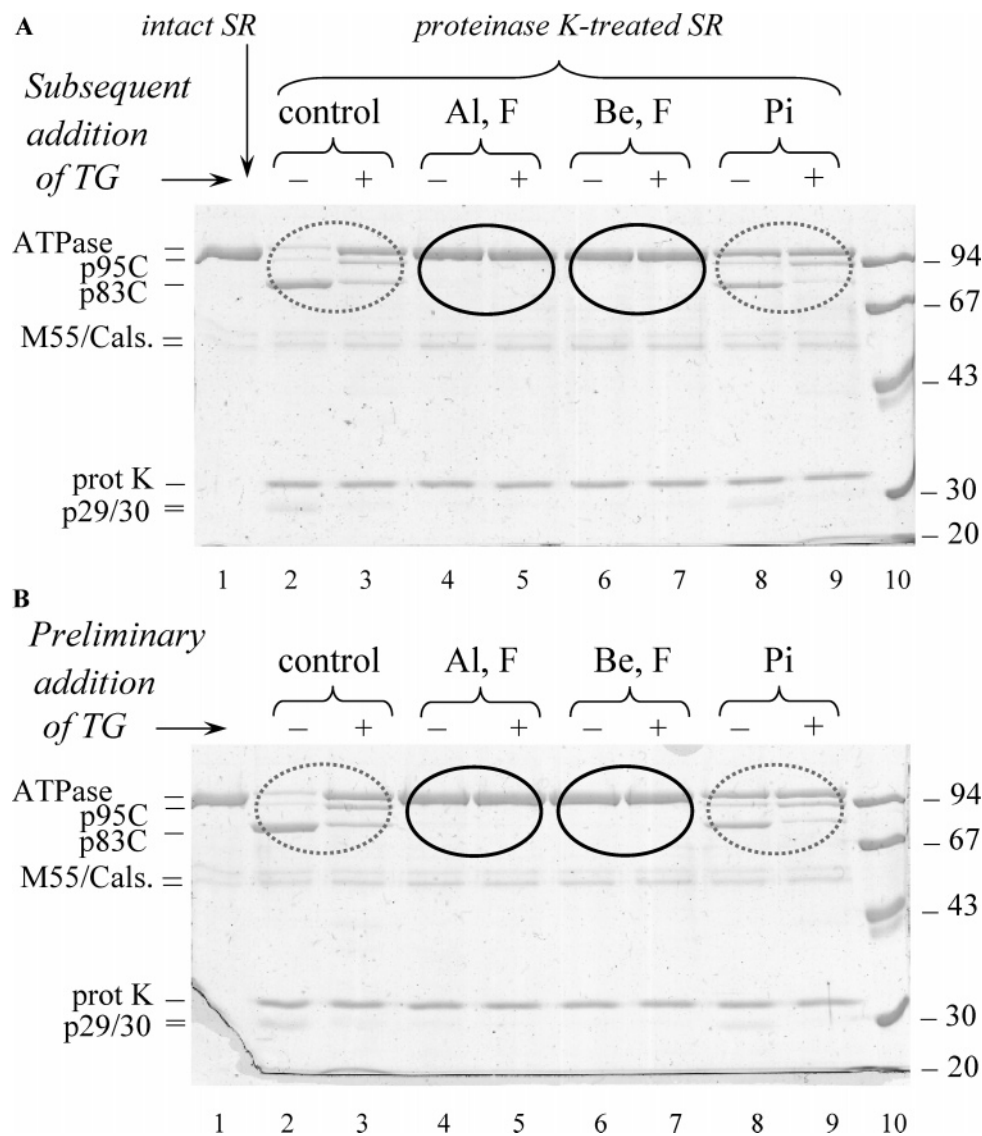


**FIGURE 1:** Fluoride-containing E2P-like forms (but not E2P itself) are fully protected from cleavage in the presence of TG *irrespective* of whether TG has been added after or before the fluoride salt, implying that the prior presence of TG does *not* prevent the ATPase from reacting with the fluoride compound. (A) SR membranes (1 mg of protein/mL) in 100 mM KCl, 20% DMSO, 150 mM Mops–Tris, 0.5 mM EGTA, and 5 mM  $Mg^{2+}$  at pH 7 and 20 °C were incubated in the absence (lanes 2 and 3) or presence of various additions: 0.05 mM  $AlCl_3$  and 1 mM KF (lanes 4 and 5), 0.05 mM  $BeCl_2$  and 1 mM KF (lanes 6 and 7), or 2 mM  $P_i$  (lanes 8 and 9). Incubation lasted 5–10 min. Similar incubations in the presence of KF and  $Mg^{2+}$  alone, KF in the absence of free  $Mg^{2+}$ ,  $BeCl_2$  without KF, or orthovanadate are shown in Figure S1 of the Supporting Information. Then, TG (0.01 mg/mL) was added to some of these samples (lanes 3, 5, 7, and 9) for 5–10 min of incubation again. Last, proteinase K was added to all samples, at 0.3 mg/mL, and proteolysis took place for 60 min. (B) Similar experiment, except that TG was added first to the  $Ca^{2+}$ -deprived SR membranes, followed after 5–10 min by fluoride (together with Al or Be) or  $P_i$  and only then, 5–10 min later, by proteinase K. In both cases, after proteolysis arrest and sample denaturation, 2  $\mu$ g of protein per lane was loaded for SDS–PAGE, here on a 9% acrylamide gel. Lanes 10 contain molecular mass markers (LMW Pharmacia kit). Lanes 1 contain intact SR (2  $\mu$ g of protein per lane, again) in the absence of proteinase K.

presence of 20% DMSO, known to stabilize formation of E2P from  $P_i$  (37).

The results illustrated in Figure 1A extend the previous results of Danko et al. to these experimental conditions and show that the ATPase indeed becomes fully resistant to proteinase K after reacting with aluminum or beryllium fluoride (a few other incubation conditions, e.g., with magnesium fluoride or vanadate, are illustrated in Figure S1 of the Supporting Information) and remains so if TG is added subsequently. TG binding under these conditions is proven by its inhibitory effect on  $Ca^{2+}$  binding to the luminal side of the ATPase (28) and also by its effects on fluorescence levels, as shown below. We also confirmed under the same conditions the more modest protective effect of  $P_i$  itself

(despite the fact that, thanks to the presence of DMSO,  $P_i$  addition here allows almost full phosphorylation), as well as the fact that this effect of  $P_i$  was disrupted by TG (35, 36). This more modest protective effect and its subsequent disruption by TG are obviously due to the dynamic nature of the E2 to E2P equilibrium, combined with the fact that TG reduces the extent of the reaction of E2 with  $P_i$  (25, 27, 38). Most importantly for our purpose, we then found that the blockade of ATPase proteolysis was independent of whether TG had been added after or *before* the fluoride salt (as shown by the identical results in panels A and B of Figure 1). This implies that the prior presence of TG does *not* prevent the cytoplasmic domains of ATPase from reacting with aluminum or beryllium fluoride in a subsequent step.



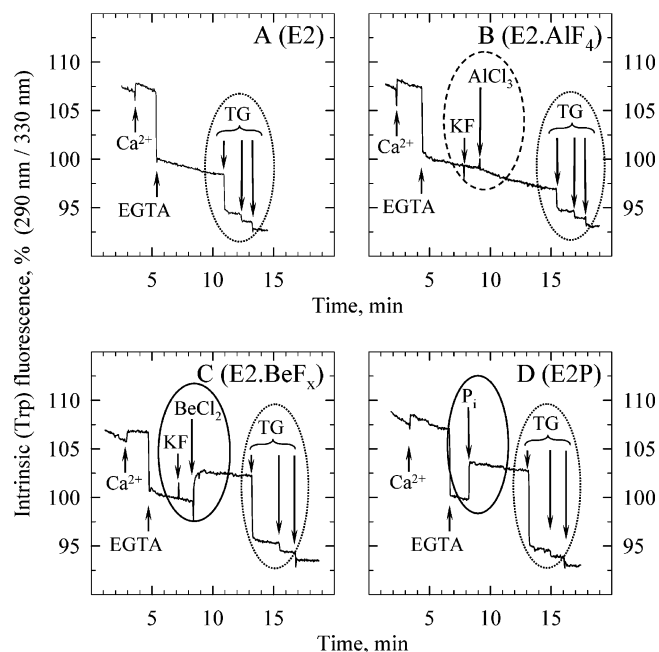


FIGURE 2: In contrast with what happens upon formation of E2·AlF<sub>4</sub> (or E2·MgF<sub>4</sub>), formation of E2·BeF<sub>x</sub> or E2P *raises* Trp fluorescence. Further addition of TG reduces it, much more for E2·BeF<sub>x</sub> or E2P than for E2·AlF<sub>4</sub> or E2, so that the final levels are similar. The fluorometer cuvette contained 0.1 mg/mL SR in 100 mM KCl, 20% DMSO, 5 mM Mg<sup>2+</sup>, and 50 mM Mops–Tris at pH 7 and 20 °C. Sequential additions were made, when indicated by arrows: Ca<sup>2+</sup> (100 μM) and EGTA (2 mM) (in all panels), KF (1 mM) and AlCl<sub>3</sub> (B) or BeCl<sub>2</sub> (C) (both at 50 μM) or P<sub>i</sub> (2 mM) (D), and last TG (1 μg/mL each addition, in all panels). The excitation wavelength was 290 nm, and the emission wavelength was 330 nm (bandwidths were 2 and 10 nm, respectively). In the various panels, the first addition of TG saturates the ATPase (1 μg/mL TG corresponds to about 1.5 μM TG, whereas 0.1 mg/mL SR corresponds to 0.5–0.7 μM ATPase), while each further addition induces an additional small quenching of fluorescence, mainly due to an inner filter effect (see also refs 25 and 36). The traces have been corrected for the (very small) artifacts induced by dilution.

From the results in ref 28 we know that adding TG (or other inhibitors) to Ca<sup>2+</sup>-free ATPase after the formation of ATPase complexes with metal fluoride prevents the normal opening of the Ca<sup>2+</sup> binding sites toward the luminal medium. To further characterize this influence of inhibitors on the ATPase transmembrane domain, we studied the consequences of TG addition on the ATPase intrinsic fluorescence, a fluorescence due to Trp residues mainly located (12 out of 13) in the transmembrane section of the ATPase. Related experiments performed in the absence of DMSO have previously been reported (36, 28), but thanks to the presence of DMSO we were here able to directly compare “E2P-like” species, formed from fluoride salts, with the “true” E2P species itself, formed from P<sub>i</sub>. Formation of the transition-state analogue E2·AlF<sub>4</sub> (from KF and AlCl<sub>3</sub>) only led to a slight relatively slow fluorescence decrease (Figure 2B), as previously found in the absence of DMSO (28). In contrast, the intrinsic fluorescence level of the ATPase rose, *both* when the E2P phosphoenzyme was formed from P<sub>i</sub> (Figure 2D) and when the E2·BeF<sub>x</sub> analogue was formed from KF and BeCl<sub>2</sub> (Figure 2C). This confirms the previous conclusion that, from the Trp fluorescence point of view, the E2·BeF<sub>x</sub> species is a much closer relative to

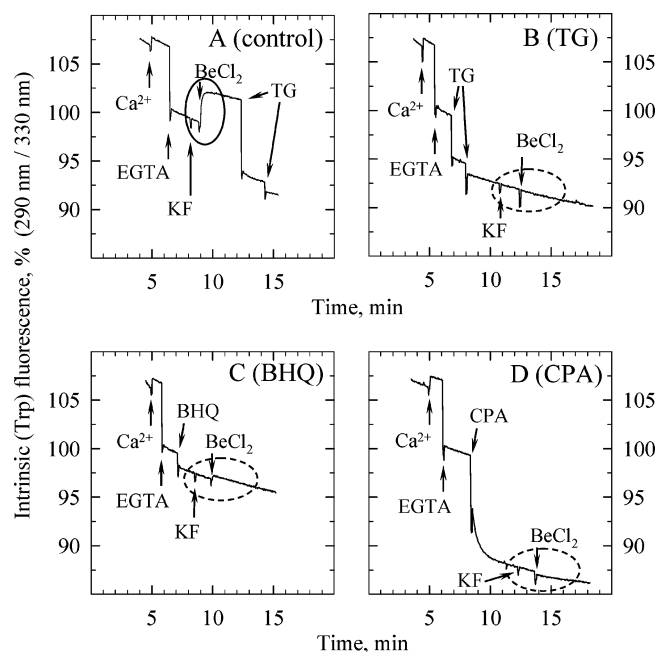


FIGURE 3: ATPase preincubation with TG, CPA, or BHQ (with poor affinity for the latter inhibitor) *prevents* the membranous Trp residues from experiencing fluorescence changes following formation of E2·BeF<sub>x</sub>. The fluorometer cuvette contained 0.1 mg/mL SR in 100 mM KCl, 20% DMSO, 5 mM Mg<sup>2+</sup>, and 50 mM Mops–Tris at pH 7 and 20 °C, as for the experiment illustrated in Figure 2. Sequential additions were made, when indicated by arrows: Ca<sup>2+</sup> (100 μM) and EGTA (2 mM) (in all panels) and then KF (1 mM) and BeCl<sub>2</sub> (50 μM) directly (A), TG (1 μg/mL, i.e., about 1.5 μM, twice) followed by KF and BeCl<sub>2</sub> (B), BHQ (30 μM) followed by KF and BeCl<sub>2</sub> (C), or CPA (0.3 μg/mL, i.e., about 1 μM) followed by KF and BeCl<sub>2</sub> (D). As for the experiment illustrated in Figure 2, the excitation wavelength was 290 nm and the emission wavelength was 330 nm (bandwidths were 2 and 10 nm, respectively). The traces have been corrected for the (very small) artifacts induced by dilution.

the true E2P state than the E2·AlF<sub>4</sub> transition-state analogue (28, 36).

Figure 2 then also shows the effect of TG addition to these various species: TG addition reduced the ATPase intrinsic fluorescence level much more for E2·BeF<sub>x</sub> or E2P than for E2·AlF<sub>4</sub> or E2, so that the final levels were not very different. Because of our proteolysis results in Figure 1, we can interpret the rather similar final fluorescence levels in the absence or presence of P<sub>i</sub> (Figure 2A,D) as simply reflecting the quasi-disappearance of E2P in the presence of TG; however, the again similar final fluorescence level in Figure 2C implies that TG addition to the ATPase complex with BeF<sub>x</sub> has modified the transmembrane region of this complex, to make it closely resemble that of the fluoride-free complex (consistent with closure of the Ca<sup>2+</sup> release channel), *despite the fact* that BeF<sub>x</sub> is *not* displaced from the cytoplasmic domains by TG.

Conversely, and to make this even more clear-cut, Figure 3 shows the result of a complementary experiment where TG was added from the start and BeF<sub>x</sub> was added at a later step only: after the prior addition of TG, subsequent addition of fluoride and beryllium no longer induced *any* change in Trp fluorescence (Figure 3B; compare with Figure 3A), although from Figure 1B we know that susceptibility to proteolysis by proteinase K is fully blocked and hence

reaction with the fluoride compound *has* occurred. In other words, upon reaction of  $\text{BeF}_x$  with the ATPase catalytic site, the transmembrane region of the ATPase complex with TG, at least as evidenced by the Trp residues, has *not* experienced any change, although one of the loops connecting the transmembrane and the cytosolic domains *has* experienced a drastic change. Similar results were obtained after reaction of ATPase with aluminum fluoride, with the same conclusion (data not shown). These results make it possible to understand that previous crystals of  $\text{Ca}^{2+}$ -free ATPase complexed with TG and fluoride salts revealed transmembrane domains pretty similar to those in the absence of fluoride, *despite* the fact that the cytosolic domains were different (8, 12, 13): TG fixes the ATPase transmembrane domain irrespective of what happens in the cytosolic domains following binding of the fluoride compound ( $\text{AlF}_4$  or  $\text{MgF}_4$  in previously published crystalline forms) and thereby may mask part of the information that would have been derived from inhibitor-free crystals.

Almost similar results were obtained using other well-characterized inhibitors of  $\text{Ca}^{2+}$ -ATPase, instead of TG, either BHQ or CPA (Figure 3C,D). In the case of BHQ, however, concentrations of BHQ much larger than stoichiometric (30  $\mu\text{M}$  in Figure 3C) were required to prevent fluorescence changes upon addition of  $\text{BeF}_x$  almost completely (2  $\mu\text{M}$  BHQ hardly changed anything, data not shown). This fits with the relatively poor affinity with which under similar conditions BHQ was found to prevent luminal opening of the  $\text{Ca}^{2+}$  binding sites (28). In contrast, and again consistent with the  $^{45}\text{Ca}^{2+}$  binding measurements in (28), CPA was effective at 1  $\mu\text{M}$ ; in this case, the fluorescence recording suggests that the binding of CPA (or the resulting blockade of transmembrane segment movements) is not instantaneous, but requires a few minutes of incubation (see also below). For both BHQ and CPA, addition of the inhibitor resulted in an apparent drop in Trp fluorescence, while as for TG, subsequent additions induced smaller drops (not shown). This is because all these inhibitors have a dual effect on ATPase intrinsic fluorescence: they perturb it by binding to the ATPase and simultaneously induce inner filter effects due to their own absorbance in the UV region (data not shown). BHQ also has some weak fluorescence itself, which counterbalances in part the inner filter effect and complicates more detailed analysis (data not shown).

**Effects of TG or Other Inhibitors on a Reporter Group (Fluorescein) at  $\text{Lys}^{515}$  in the Nucleotide Binding Domain.** From the above results, we concluded that in the presently available crystals where  $\text{Ca}^{2+}$ -free ATPase is complexed with  $\text{AlF}_4$  or  $\text{MgF}_4$  and TG, TG has probably driven the ATPase transmembrane domain into a fixed state irrespective of what had happened in the cytosolic domains following binding of the fluoride compound (see, e.g., refs 8, 12, and 13). One question, then, is to which extent, in these crystals, TG could have altered the organization of the cytosolic domains too, despite the fact (Figure 1) that ATPase reaction with the fluoride compound had remained possible. To address this issue, we explored the response to the addition of TG of an extrinsic label located in the cytosolic region, namely, FITC bound at  $\text{Lys}^{515}$  in the nucleotide binding domain. TG has already been reported to block the FITC fluorescence changes induced by  $\text{Ca}^{2+}$  addition or removal, but reports of the effect of TG per se on FITC fluorescence are scarce in the literature

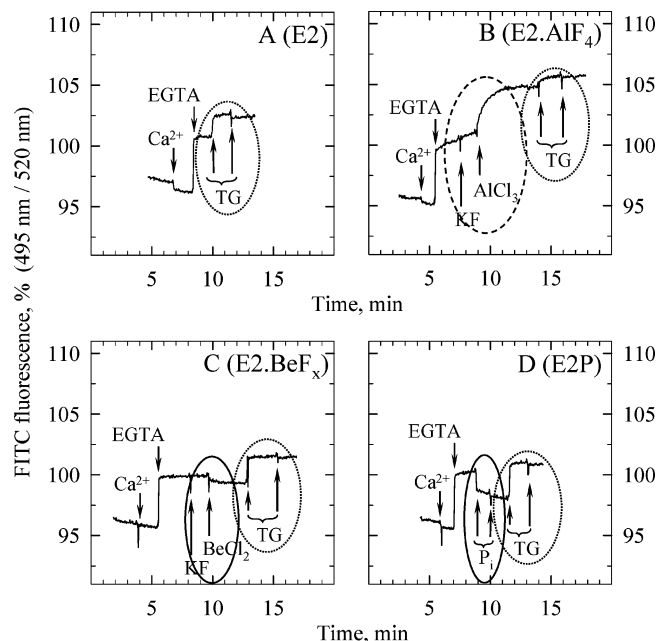


FIGURE 4: In  $\text{E2}\cdot\text{BeF}_x$  (or  $\text{E2P}$ ), the fluorescence of FITC bound to  $\text{Lys}^{515}$  differs from that in  $\text{E2}\cdot\text{AlF}_4$  (or  $\text{E2}\cdot\text{VO}_4$ , not shown). FITC fluorescence hardly responds to TG addition to  $\text{E2}\cdot\text{AlF}_4$  (or  $\text{E2}\cdot\text{VO}_4$ ) but responds quite significantly to TG addition to  $\text{E2}\cdot\text{BeF}_x$ . The fluorometer cuvette contained 0.02 mg/mL FITC-SR in 100 mM KCl, 20% DMSO, 5 mM  $\text{Mg}^{2+}$ , and 150 mM Mops-Tris at pH 7 and 20 °C. Sequential additions were made, when indicated by arrows:  $\text{Ca}^{2+}$  (20  $\mu\text{M}$ ) and EGTA (0.2 mM) (in all panels), KF (1 mM) and  $\text{AlCl}_3$  (B) or  $\text{BeCl}_2$  (C) (both at 50  $\mu\text{M}$ ) or  $\text{P}_i$  (2 mM, followed by another identical addition of 2 mM) (D), and TG (1  $\mu\text{g}/\text{mL}$  each addition, in all panels). The excitation wavelength was 495 nm, and the emission wavelength was 520 nm (bandwidths were 2 and 10 nm, respectively). In the various panels, the first addition of TG saturates the ATPase. The traces have been corrected for the (small) artifacts induced by dilution. Effects of TG addition to the  $\text{E2}\cdot\text{VO}_4$  species are shown in Supporting Information Figure S2.

(see, e.g., refs 25 and 66).

As a preliminary result, under the exact same conditions as those documented above, i.e., in the presence of DMSO and KCl at pH 7, Figure 4 first shows the previously undocumented fact that the response of FITC fluorescence to ATPase reaction with  $\text{BeF}_x$  is a drop in FITC fluorescence (Figure 4C), similar in sign to its response to ATPase reaction with  $\text{P}_i$  (Figure 4D, a previously undocumented drop too), whereas ATPase reaction with  $\text{AlF}_4$  triggers a response of opposite sign (Figure 4B, a rise in FITC fluorescence, rather similar to that classically observed (39) upon ATPase reaction with another putative transition state, orthovanadate; see Supporting Information Figure S2A). Thus, the  $\text{E2}\cdot\text{BeF}_x$  species again appears to be more similar to the true  $\text{E2P}$  species than to the  $\text{E2}\cdot\text{AlF}_4$  or  $\text{E2}\cdot\text{VO}_4$  species. When TG was added to the FITC-labeled  $\text{E2}\cdot\text{BeF}_x$  species, FITC fluorescence rose quite significantly (Figure 4C); in contrast, there was only a slight change upon addition of TG to  $\text{E2}\cdot\text{AlF}_4$  (Figure 4B) (while TG addition to  $\text{E2P}$  (Figure 4D) increased FITC fluorescence back to the level found in the absence of  $\text{P}_i$  (Figure 4A), as expected from the dynamic nature of phosphorylation from  $\text{P}_i$ ).

From these results, we may infer that the ATPase structure around  $\text{Lys}^{515}$  in the previously published TG· $\text{E2}\cdot\text{AlF}_4$  crystals (13) probably did *not* suffer much from the presence of TG, but the ATPase structure in a putative TG· $\text{E2}\cdot\text{BeF}_x$

crystal, if such a structure were to become available, might deviate more significantly, even in the cytosolic region, from its TG-free counterpart, again assuming the latter could also become available. It is however fair to recall that in previous experiments where TNP-AMP bound in the cytosolic domain, instead of FITC, was used as the reporter group, addition of TG to the  $E2 \cdot BeF_x$  species left hydrophobicity around the TNP group essentially unaltered (36); thus, those results with TNP-AMP point to the possibility that the effect of TG on the cytosolic domains suggested by our FITC data might remain rather limited. Nevertheless, consistent with a general effect of TG at the nucleotide binding site (where the fluorescein is located), it may be recalled that TG is known to reduce the ATPase affinity for MgATP (14, 40–42; see also below).

Focusing on the  $E2 \cdot VO_4$  and  $E2 \cdot AlF_4$  species, whose formation is most clearly revealed by the fluorescein reporter group, formation of these species was not prevented by the preliminary addition of TG (Supporting Information Figure S2C,D), consistent with the proteolysis results. This was true also in the absence of DMSO (Supporting Information Figure S3), i.e., under conditions where the fluorescence rise associated with  $VO_4$  binding has been extensively described (39). Note that TG-dependent and  $VO_4$ -dependent FITC signals are significantly larger in the absence than in the presence of DMSO (as shown by comparing Figure S3A with Figure S2A and Figure S3C with Figure S2C), which makes the former conditions more favorable to study the effects of TG or  $VO_4$  on FITC fluorescence. Other inhibitors influenced FITC fluorescence in a manner qualitatively similar to that of TG: they all increased the basic fluorescence level of FITC but did not prevent formation of the transition-state analogue (Supporting Information Figure S4). BHQ was again less effective than TG or CPA, as at a concentration of a few micromolar it blocked the effect of subsequent addition of  $Ca^{2+}$  only partially.

*Effects of TG or Other Inhibitors on Other Forms of  $Ca^{2+}$ -Free ATPase, As Deduced from Intrinsic Fluorescence Responses to  $Mg^{2+}$  or ATP.* We then explored the effect of TG, BHQ, and CPA on two other events: binding of  $Mg^{2+}$  and ATP to  $Ca^{2+}$ -free ATPase. These two events are known to give rise to distinct Trp fluorescence changes, which were observed here in the absence of DMSO and KCl. The Trp fluorescence changes accompanying  $Mg^{2+}$  addition at neutral or alkaline pH (43) were completely obliterated in the presence of TG (part A versus part B of Figure 5). This was also essentially true in the presence of BHQ at 10  $\mu$ M (Figure 5C), but again BHQ appeared to bind with relatively poor affinity, as the rate of its dissociation upon subsequent addition of excess  $Ca^{2+}$  was much faster than for TG (at only 3  $\mu$ M BHQ, Trp fluorescence remained sensitive to  $Mg^{2+}$  and the rate of the subsequent  $Ca^{2+}$ -induced rise was faster than at 10  $\mu$ M BHQ, while at 30  $\mu$ M BHQ, this rate was slowest, data not shown). In the presence of CPA, it turned out that addition of  $Mg^{2+}$  after CPA induced a further drop in Trp fluorescence (Figure 5D): this peculiar feature probably reveals that CPA itself binds tighter (or to a larger extent) to the ATPase at millimolar concentrations of  $Mg^{2+}$  than at the micromolar concentration found in nominally  $Mg^{2+}$ -free buffer and hence is more efficient in quenching Trp fluorescence (see the Discussion).

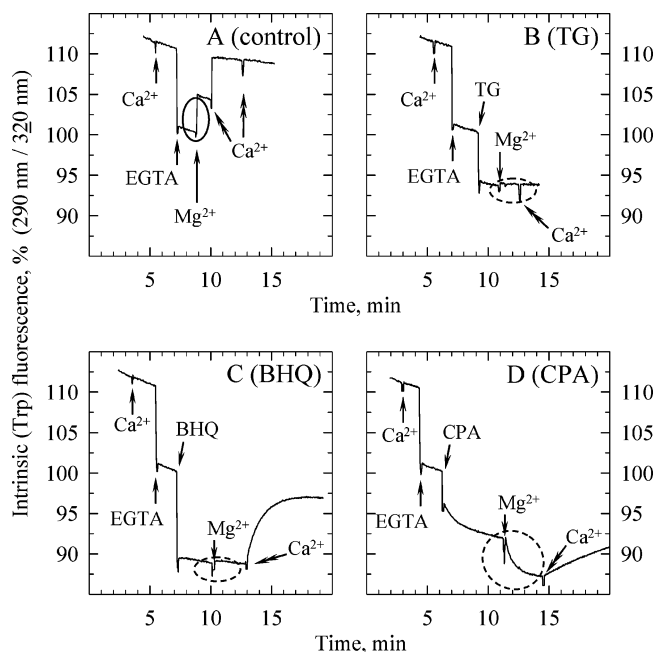
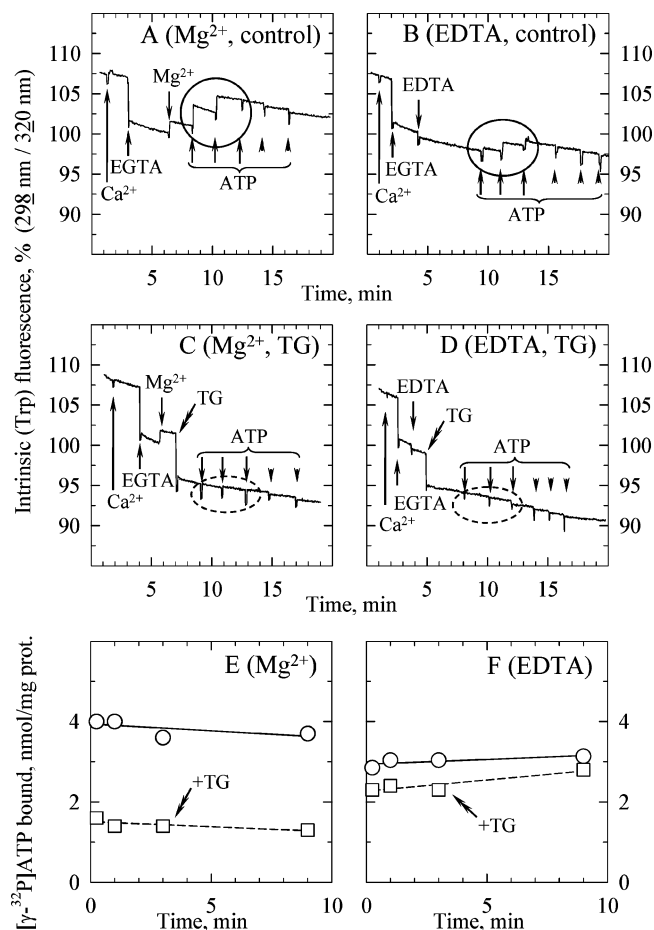


FIGURE 5: TG (as well as BHQ) completely obliterates the response of ATPase Trp residues to the addition of  $Mg^{2+}$  to  $Ca^{2+}$ -free ATPase. The response to  $Mg^{2+}$  in the presence of CPA is masked by enhanced CPA interaction with the ATPase following addition of  $Mg^{2+}$ . The fluorometer cuvette contained 0.1 mg/mL SR in 150 mM Mops-Tris at pH 7 and 20 °C. Sequential additions were made as follows, when indicated by arrows:  $Ca^{2+}$  (100  $\mu$ M), EGTA (1 mM), inhibitor if any [in panel B TG (1  $\mu$ g/mL), in panel C BHQ (10  $\mu$ M), and in panel D CPA (0.3  $\mu$ g/mL)], then  $Mg^{2+}$  (20 mM), and last (double arrow)  $Ca^{2+}$  again (at 1 mM, added twice in panel A, which is the control). The excitation wavelength was 290 nm, and the emission wavelength was changed to 320 nm to optimize the  $Mg^{2+}$ -dependent signal (43); bandwidths were 2 and 10 nm, respectively. This experiment was performed at pH 7 in the absence of KCl, but similar results were also obtained at pH 7.5 (which further optimizes the  $Mg^{2+}$ -dependent signal; see ref 43) or at pH 7 but in the additional presence of 100 mM KCl (which slightly depresses it, unpublished results). Traces have been corrected for the (small) artifacts induced by dilution.

We then studied the effects of inhibitors on the Trp fluorescence changes that normally accompany ATP addition to  $Ca^{2+}$ -free ATPase (44, 45, 34, 19). In the presence of  $Mg^{2+}$ , where the affinity for ATP (MgATP, in fact) is high in the absence of TG, TG completely inhibited these fluorescence changes (Figure 6A,C), a fact which was previously noted (46) but only briefly commented upon as reflecting the known TG-induced drop in the affinity of the ATPase for MgATP (46, 41, 67). Remarkably, however, this was also the case in the total absence of free  $Mg^{2+}$  (Figure 6B,D), i.e., under conditions where the binding of ATP (with poorer affinity) has been suggested to be almost unaltered by TG (47). In relation with that suggestion, and because of the existence of seemingly contradictory results obtained under different ionic conditions (14), we performed [ $\gamma$ - $^{32}P$ ]-ATP binding experiments under our ionic conditions (using a filtration assay), and we were able to confirm the suggestion in ref 47: at the relatively high concentration of [ $\gamma$ - $^{32}P$ ]ATP we used (30  $\mu$ M), i.e., with the ATPase nucleotide binding site essentially fully saturated in the presence of  $Mg^{2+}$  and only partially in the absence of  $Mg^{2+}$ , TG hardly affected the amount of ATP bound in the absence of  $Mg^{2+}$  (and the amount of ATP bound to the ATPase-TG complex was in fact higher in the absence of  $Mg^{2+}$  than in its presence;





**FIGURE 6:** TG completely obliterates the response of ATPase Trp residues to the residual binding of either MgATP or ATP. (A–D) The fluorometer cuvette contained 0.1 mg/mL SR in 150 mM Mops–Tris at pH 7 and 20 °C. Sequential additions were made as follows, when indicated by arrows: Ca<sup>2+</sup> (100  $\mu$ M), EGTA (1 mM), Mg<sup>2+</sup> (5 mM; A, C) or EDTA (2 mM; B, D), and TG if any (1  $\mu$ g/mL; C, D); then, increasing concentrations of ATP were added, 3  $\mu$ M first, then 30  $\mu$ M more, then 300  $\mu$ M more, and last two or three additions of 300  $\mu$ M again (arrowheads). The excitation wavelength was set at 298 nm to reduce the inner filter effect due to ATP absorbance, while the emission wavelength was kept at 320 nm; bandwidths were 2 and 10 nm, respectively. Traces have been corrected for the (very small) artifacts induced by dilution. (E, F)  $[\gamma\text{-}^{32}\text{P}]\text{ATP}$  binding to the ATPase (in the presence of 30  $\mu$ M ATP) under almost exactly the same conditions, as deduced from filtration experiments. At time zero, 30  $\mu$ M  $[\gamma\text{-}^{32}\text{P}]\text{ATP}$  was added to Ca<sup>2+</sup>-free ATPase (0.1 mg/mL), suspended in 150 mM Mops–Tris (pH 7 and 20 °C), 0.5 mM EGTA, and either 5 mM Mg<sup>2+</sup> (E) or 0.5 mM EDTA (F), and preincubated in the absence (circles) or presence (squares) of 1  $\mu$ g/mL TG. After various periods, 2.5 mL aliquots were filtered on Millipore HA filters and double-counted without rinsing. In panel E, the tendency for bound ATP to become slightly lower after long periods most probably reveals Mg<sup>2+</sup>-dependent ATP hydrolysis by contaminant enzymes.

see the squares in part F versus part E of Figure 6). Both in the presence and in the absence of Mg<sup>2+</sup>, the amount of bound ATP remained significant in the presence of TG. Thus, the total absence of ATP-induced fluorescence changes under any of these two conditions implies that TG completely prevented the Trp residues in the membrane from experiencing any distinct change in environment upon the residual binding of ATP to the ATPase cytosolic domain: ATP still binds to the ATPase (with modest affinity) despite the presence of TG, but (as previously observed after formation

of an E2•BeF<sub>x</sub> complex) no longer induces any conformational change in the transmembrane domain, where most of the Trp residues are located.

Similar experiments were repeated using BHQ or CPA instead of TG. BHQ proved to act very similarly to TG, although again with poorer affinity. In the presence of Mg<sup>2+</sup>, 30  $\mu$ M BHQ nearly completely prevented (Supporting Information Figure S5A) the normal response of ATPase Trp residues to MgATP addition previously illustrated in Figure 6A, although about half of the  $[\gamma\text{-}^{32}\text{P}]\text{ATP}$  remained bound in the presence of BHQ (Figure S5E); 10  $\mu$ M BHQ was not sufficient in the presence of Mg<sup>2+</sup> (data not shown). In the absence of Mg<sup>2+</sup>, 10  $\mu$ M BHQ was sufficient to eliminate the fluorescence response to ATP addition (compare Figure S5B with its control in Figure 6B), although  $[\gamma\text{-}^{32}\text{P}]\text{ATP}$  binding was only minimally altered by BHQ (Figure S5F). CPA revealed specific features, to be considered in parallel with its previously noted specific behavior in the experiments illustrated in Figures 3D and 5D. In the absence of free Mg<sup>2+</sup>, addition of CPA no longer induced any observable time-dependent fluorescence response, and the rapid fluorescence drop observed now matched exactly the drop expected for an inner filter effect alone (Supporting Information Figure S5D); the binding of  $[\gamma\text{-}^{32}\text{P}]\text{ATP}$  to ATPase was again minimally altered by CPA (Figure S5F), but in this case the accompanying fluorescence changes, too, were minimally altered (compare Figure S5D with its control in Figure 6B); thus, CPA seems to hardly interact with the ATPase in the absence of Mg<sup>2+</sup>. In the presence of Mg<sup>2+</sup>, the time-dependent fluorescence drop, which we believe to be a manifestation of CPA interaction with the ATPase, was completed on a time scale of minutes (Figure S5C). After this equilibration, addition of ATP (i.e., MgATP) no longer induced any fast rise in Trp fluorescence, as for TG or BHQ, despite the reduced but again nonzero amount of  $[\gamma\text{-}^{32}\text{P}]\text{ATP}$  bound after short periods (Figure S5E; see also ref 67). At later times, Trp fluorescence rose slowly (compare Figure S5C with its control in Figure 6A), possibly revealing slow displacement of CPA from its binding site(s) (as also found in Figure 5D) concomitant with a slow increase in the amount of bound  $[\gamma\text{-}^{32}\text{P}]\text{ATP}$  (Figure S5E).

**Effects of TG or Other Inhibitors on Ca<sup>2+</sup>-Free ATPase in the Absence of Any Other Ligand, As Deduced from Mild Proteolysis Experiments with Proteinase K.** Last, we studied the effects of inhibitors on Ca<sup>2+</sup>-free ATPase in the absence of any other ligand, by using the ATPase susceptibility to proteinase K as an indicator of possible changes in its conformation or dynamics. To be consistent with the experiments in Figures 5 and 6, we chose here to keep proteolysis media devoid of DMSO and KCl; compared with the previous proteolysis experiments illustrated in Figure 1, we had to use a lower proteinase K to SR membrane ratio in the new experiments, because both DMSO and KCl appear to slow ATPase proteolysis (Figure S6 in the Supporting Information). As an introduction to these experiments, let us first recall (30, 48) that, during mild treatment of SR vesicles with proteinase K in the presence of Ca<sup>2+</sup>, a number of well-characterized initial products are formed, including membranous peptides derived from either the C-terminal (p83C, p27/28C, and p19C) or the N-terminal (p28N and a small amount of p81N) part of the ATPase, as well as water-soluble p29/30 fragments derived from the



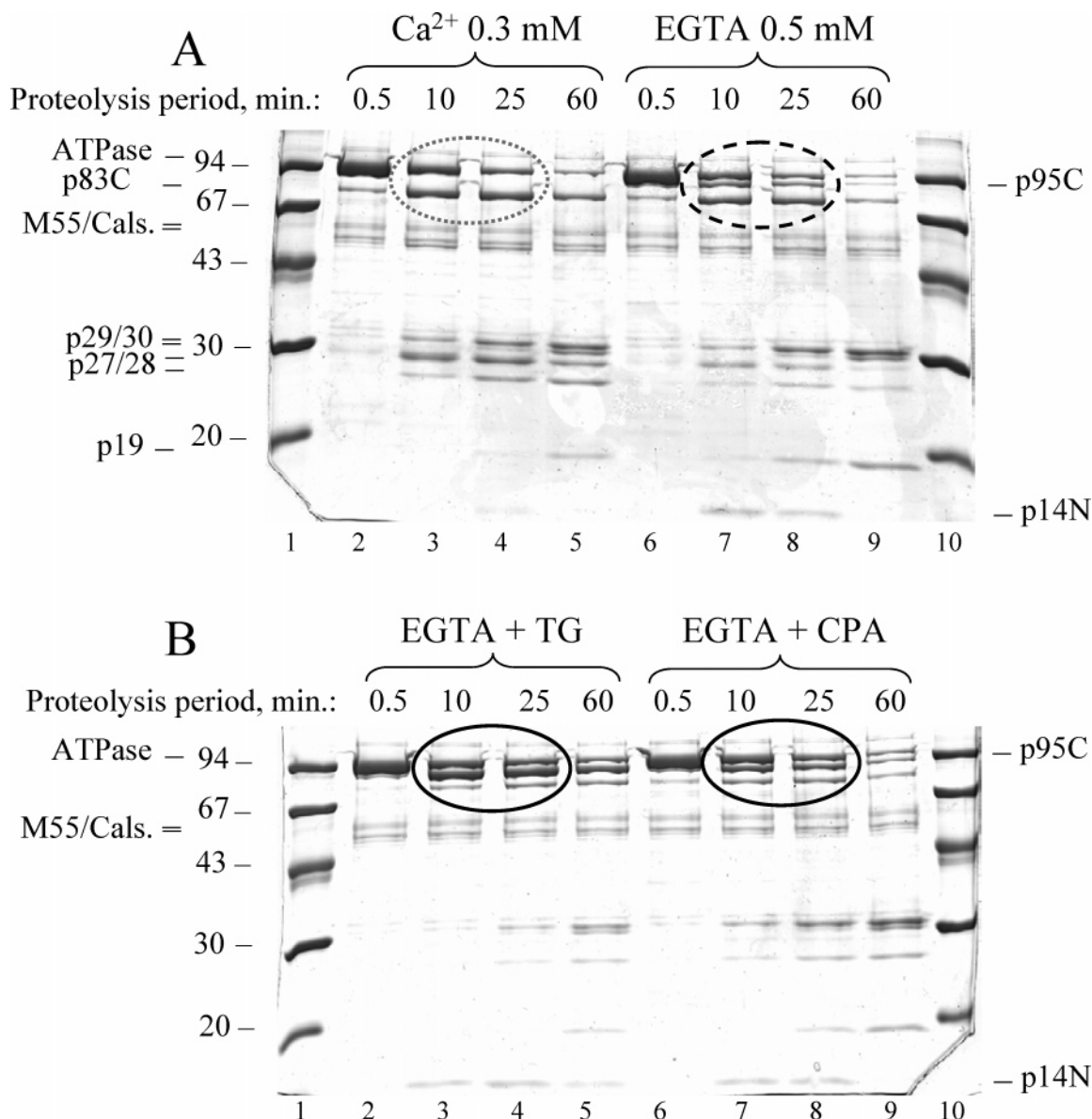


FIGURE 7: The presence of TG (or CPA) during proteinase K treatment of  $\text{Ca}^{2+}$ -free ATPase slows cleavage at T242–E243, resulting in the formation of large amounts of p95C. (A) SR membranes (2 mg of protein/mL) were treated with proteinase K (0.03 mg/mL) at 20 °C for various periods of time, in proteolysis buffer (100 mM Mops–NaOH and 5 mM  $\text{Mg}^{2+}$  at pH 6.5) containing either 0.3 mM  $\text{Ca}^{2+}$  (lanes 2–5) or 0.5 mM EGTA (lanes 6–9). After proteolysis arrest and sample denaturation, 4  $\mu\text{g}$  of protein was loaded per lane, on a 12% acrylamide gel. Lanes 1 and 10 contain molecular mass markers (LMW kit, GE Healthcare). This is a repeat of the experiment illustrated in Figure 1A of ref 49, but performed exactly in parallel with the one illustrated in panel B. (B) SR membranes were similarly treated in the presence EGTA, except for the additional presence of either TG (lanes 2–5) or CPA (lanes 6–9), both at 20  $\mu\text{g}/\text{mL}$  (i.e., about 30  $\mu\text{M}$  for TG and 60  $\mu\text{M}$  for CPA; 2 mg/mL SR corresponds to about 10–14  $\mu\text{M}$  ATPase, assuming 5–7 nmol of ATPase/mg of protein).

central and cytosolic nucleotide binding domain (see lanes 2–5 in gel A of Figure 7, corresponding to an experiment performed at pH 6.5). The C-terminal peptide p83C results from ATPase cleavage at T242–E243, and the T242–E243 bond is indeed peripheral (and therefore accessible to proteolysis) in the structure of the  $\text{Ca}^{2+}$ -bound form of  $\text{Ca}^{2+}$ –ATPase (7). In the absence of  $\text{Ca}^{2+}$ , as seen by lanes 6–9 in gel A, a new high molecular mass peptide is also formed (compare lanes 6–9 with lanes 2–5; see also Figure 1 in ref 49): this p95C peptide, a C-terminal one, is formed together with its N-terminal counterpart, p14N, after ATPase cleavage at L119–K120 (30).

Similar experiments were repeated in the absence of  $\text{Ca}^{2+}$  but now in the presence of TG. TG was previously described to only moderately slow overall proteolysis of the initial

ATPase (35). We confirmed this, but in addition we found that the presence of TG has a clear qualitative effect on the pattern of proteolysis: p83C becomes much weaker, while p95C is now predominant (lanes 2–5 in gel B versus lanes 6–9 in gel A of Figure 7). In Danko et al.'s previous paper (35), the same qualitative trend (although less pronounced under the conditions of that paper) is also visible (see Figure 2 in ref 35), and a similar TG-induced inversion of the p83 to p95 ratio has been reported in Western blots (50, 67). We also found that the presence of CPA, instead of TG, during proteolysis in the presence of EGTA, exerts effects on formation of p95C and p83C that are qualitatively similar to those exerted by TG, although slightly less pronounced (Figure 7B, lanes 6–9): the overall loss of intact ATPase is again slowed, and the formation of p95C is again favored at

the expense of p83C. The same result, including the fact that the effect was weaker, was found when BHQ was used (Figure S7 in the Supporting Information). The more prominent p95C band and the reduced p83C band, in the presence of TG or the other inhibitors, must be due to a slowing of the cut at T242–E243 rather than to stimulation of the cut at L119–K120, as disappearance of intact ATPase is *slower* in the presence of inhibitors than in their absence (i.e., in the absence of inhibitors, formation of the p95C peptide in the absence of  $\text{Ca}^{2+}$  is underestimated because cleavage at T242–E243 also occurs). Thus, we conclude that TG, BHQ, and CPA all reduce the rate of cleavage at T242–E243, with the effect of BHQ or CPA being slightly less pronounced.

A conceivable interpretation for this inhibitor-induced alteration in the proteolysis pattern might be that  $\text{Ca}^{2+}$ -free ATPase explores various conformations, only a few of which correspond to the true E2 conformation, with this true conformation, defined as being the conformation reactive to  $\text{P}_i$ , being the only one able to bind TG (25, 26, 40, 51). It has indeed already been suggested that  $\text{Ca}^{2+}$ -free ATPase is in dynamic equilibrium between a true “E2” state and a  $\text{Ca}^{2+}$ -free “E1” state (partly resembling the  $\text{Ca}^{2+}$ -saturated ATPase conformation) (39). However, the E2/E1 equilibrium is generally thought to depend on the pH (and temperature), being about 50/50 under neutral conditions at 20 °C, but being almost fully shifted toward the E2 form under more acidic conditions (39), partly because the E2 species corresponds to a form in which protons (to be countertransported for  $\text{Ca}^{2+}$ ) are bound and occluded (52); it was recently suggested explicitly that, at pH 6, TG could stabilize the ATPase in the protonated “ $\text{H}_n\text{E2}$ ” state (14).

To test this interpretation, we repeated our experiments under different pH conditions. We predicted that if TG were merely stabilizing a pre-existing protonated E2 form, the effect of TG on susceptibility to proteolysis would be minimal at pH 6 (where the E2/E1 equilibrium is already shifted toward the E2 state in the absence of TG) but prominent at pH 7 (where half of the  $\text{Ca}^{2+}$ -free ATPase is in the  $\text{Ca}^{2+}$ -free E1 state in the absence of TG). However, the result of the experiment did not fit with this prediction: the effect of TG on ATPase susceptibility to proteolysis in the absence of  $\text{Ca}^{2+}$  was prominent *both* at pH 6 (Figure 8A) and at pH 7 (Figure 8B), and the p95C to p83C ratio in the absence of TG was even lower at pH 6 than at pH 7, so that the relative effect of TG was even stronger at pH 6 than at pH 7. Whether this result fits better or not with the alternative and previously proposed possibility (53–55) that, irrespective of pH, TG (as well as other inhibitors such as BHQ or CPA) drives the ATPase toward a state that somehow *differs* from that of inhibitor-free ATPase, will be discussed below.

## DISCUSSION

At present, due to the known instability of detergent-solubilized  $\text{Ca}^{2+}$ -free forms of ATPase, the diffracting crystals we have for some of these forms of ATPase were all obtained in the presence of inhibitors (mostly TG, but also BHQ or CPA). These forms (with or without fluoride, for instance) do differ in their cytosolic regions, but for a given type of inhibitor (TG for instance) they have rather

similar organizations in their transmembrane domain. The likely reason for the latter fact is now made clear by our results: TG does not prevent a number of events from occurring in the ATPase cytosolic domain, e.g., reaction with fluoride compounds (Figure 1B) or binding of ATP with reduced affinity (Figure 6E,F), but it apparently prevents the transmembrane helices from responding to these cytosolic events (Figures 3 and 6A–D). Thus, the present work emphasizes that, to better understand the various conformations of sarcoplasmic reticulum ATPase during its catalytic cycle, especially its  $\text{Ca}^{2+}$ -free forms, we do need crystals prepared in the *absence* of inhibitor. Indeed, from the beginning, TG was considered as a “dead-end complex” (25), and as was explicitly stated a few years later after directed mutagenesis and chimeric exchange experiments, “perturbations produced by binding of either inhibitor within the stalk segment interfere with the long-range functional linkage between ATP utilization in the ATPase cytosolic region and  $\text{Ca}^{2+}$  binding in the membrane-bound region” (56). Here, we have demonstrated this directly with native sarcoplasmic reticulum ATPase. Although we are not able to exactly pinpoint the nature of the perturbations exerted by the inhibitors, we show that, beyond the transmembrane region, they extend to the loop(s) connecting this region and the cytosolic domains (Figures 7 and 8) and even higher above the membrane, up to fluorescein bound to  $\text{Lys}^{515}$  in the nucleotide binding domain (Figure 4); the effects of TG on the headpiece of  $\text{Ca}^{2+}$ -free ATPase were in fact predicted (67). All this should be kept in mind when the structures of the forms obtained in the presence of TG or other inhibitors are considered. This *caveat* holds especially for the ATPase crystalline forms obtained with fluoride compounds ( $\text{TG} \cdot \text{E2} \cdot \text{MgF}_4$ , or  $\text{TG} \cdot \text{E2} \cdot \text{AlF}_4$ ), which at present are the only analogues available for the true E2P form but still differ from it or from its closest relative, the TG-free  $\text{E2} \cdot \text{BeF}_x$  form (Figures 2 and 4), both in the transmembrane domain (Figure 3 and ref 28) and probably in the nucleotide domain too (Figure 4C). However, it possibly holds also for the ATPase forms obtained in the presence of nucleotide and inhibitors, as TG apparently blocks long-distance reorganization by nucleotides of the ATPase transmembrane domain, even though nucleotide binding still takes place (Figure 6 and Supporting Information Figure S5).

Our results about the effect of  $\text{Mg}^{2+}$  binding to  $\text{Ca}^{2+}$ –ATPase—at least as concerns the particular type of  $\text{Mg}^{2+}$  binding which results in Trp fluorescence changes observable under neutral or alkaline conditions—may also be discussed. The exact reason for this effect of  $\text{Mg}^{2+}$  has been disputed from the start. One of the possibilities is that this  $\text{Mg}^{2+}$  ion could bind to one of the two  $\text{Ca}^{2+}$  sites, resulting in a shift of the ATPase conformation toward a  $\text{Ca}^{2+}$ -free but “E1-like” new conformation (43, 57). In this case, the blockade of the effect of  $\text{Mg}^{2+}$  by TG would indeed be easily understandable. However, Trp fluorescence experiments with the E309Q mutant (mutated at  $\text{Ca}^{2+}$  binding site “II”) showed that  $\text{Mg}^{2+}$  was able to bind to this mutant and to induce normal fluorescence changes, although  $\text{Ca}^{2+}$  was no longer able to induce such changes (58); thus, in that work, it was suggested that  $\text{Mg}^{2+}$  was *not* binding at any of the  $\text{Ca}^{2+}$  sites in the transmembrane region. If this is correct, the binding site for  $\text{Mg}^{2+}$  (at least for this  $\text{Mg}^{2+}$  ion) could then be between  $\text{Asp}^{703}$  and  $\text{Asp}^{707}$  in the catalytic site, as observed

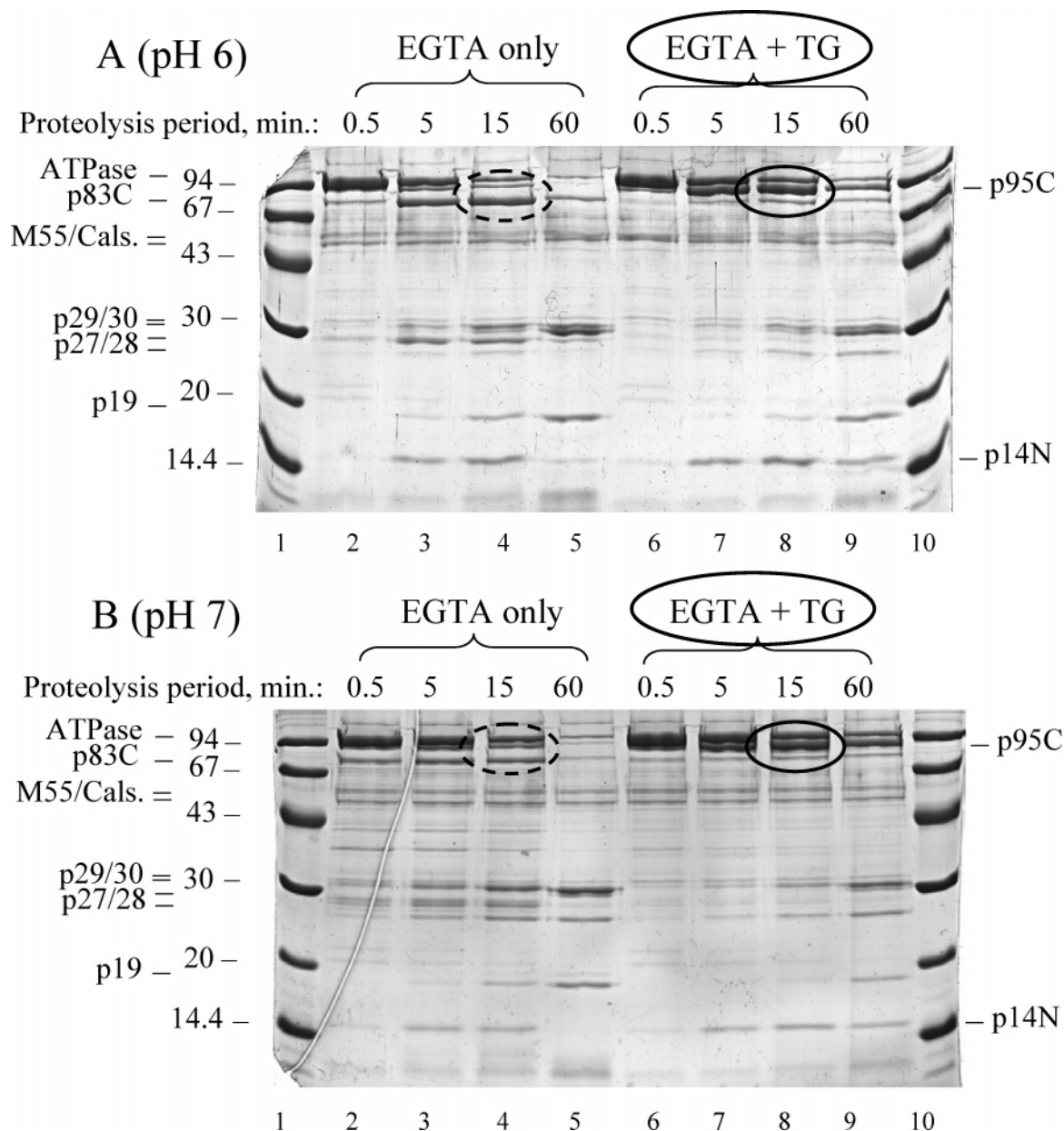


FIGURE 8: At both pH 6 and pH 7, the presence of TG in the absence of  $\text{Ca}^{2+}$  blocks ATPase cleavage by proteinase K at T242–E243 almost fully, resulting in overwhelming formation of the p95C peptide. SR membranes were treated as described in Figure 7 in the presence of 5 mM  $\text{Mg}^{2+}$  and 0.5 mM EGTA and the absence (lanes 2–5) and presence (lanes 6–9) of 0.02 mg/mL TG, but now in a medium consisting of either 50 mM Mes–Tris at pH 6 (A) or 50 mM Mops–Tris at pH 7 (B). After proteolysis arrest and sample denaturation, 4  $\mu\text{g}$  of protein was loaded per lane, on a 12% acrylamide gel.

in a recently obtained E2(TG)AMPPCP crystal (PDB structure deposited as 2DQS, to be commented upon elsewhere), and the Trp response to  $\text{Mg}^{2+}$  would reveal  $\text{Mg}^{2+}$ -induced long-distance reorganization (in the absence of inhibitor) of the transmembrane region of the ATPase, and again this long-distance reorganization would turn out to be blocked by TG. However, at variance with the suggestion in ref 58, it is fair to recognize that site II of E309Q might have retained the ability to bind  $\text{Mg}^{2+}$  even though it has lost the ability to bind  $\text{Ca}^{2+}$ . Thus, a firm conclusion about the exact site to which  $\text{Mg}^{2+}$  has to bind to induce Trp fluorescence changes must probably be delayed until experiments with other mutants have been performed.

The results obtained with ATP and MgATP may also be shortly discussed here. Although, as well-known, TG affects the binding of MgATP very significantly, we confirmed that,

as recently described (47), TG affects the binding of ATP in the absence of  $\text{Mg}^{2+}$  to a very slight extent only; it was previously known, too, that TG hardly affects the binding of ATP analogues such as TNP–ATP (46) or TNP–8N<sub>3</sub>–ATP (41). MgATP and ATP might in fact bind in slightly different conformations (59), and a complex of  $\text{Ca}^{2+}$ -free ATPase with TG might conceivably bind nucleotides (e.g., AMP–PCP) in a still somewhat different conformation.

Our results also add a few details to the characterization of the effect of BHQ and CPA. As concerns BHQ, our results confirm that this inhibitor binds with relatively poor affinity (in the range of a few micromolar in most of our experiments), but otherwise acts rather similarly to TG. In likely relation with this, the structure of the ATPase in BHQ·ATPase crystals was not found to be very different from that in the presence of TG (17). As concerns CPA, we deduce



from the Trp fluorescence results (Figures 3D, 5D, and S5C) that it reorganizes the transmembrane domain with kinetics which is not very fast (on the minute time scale in the presence of  $\text{Mg}^{2+}$ ), compared with the much faster kinetics with which TG and BHQ act (54, 60). However, we also suspect that the mere binding of CPA to ATPase might depend on  $\text{Mg}^{2+}$  availability (part C versus part D of Supporting Information Figure S5). Similarly, partition of the well-known ionophore calcimycin (A23187) into sarcoplasmic reticulum membranes (see, e.g., ref 61) is favored by millimolar concentrations of  $\text{Mg}^{2+}$  (unpublished data).

As concerns the effects of inhibitors on the proteolytic susceptibility of ligand-free ATPase (at least using proteinase K as the protease), our similar results at different pH values (Figure 8) might at first sight be taken as rendering less likely the possibility that inhibitors could stabilize the true E2 conformation of the pump, the true E2 conformation being defined as the dynamic ensemble of conformations making the ATPase reactive to  $\text{P}_i$ , as opposed to the " $\text{Ca}^{2+}$ -free E1" conformation which, in  $\text{Ca}^{2+}$ -free ATPase, is in a pH-dependent equilibrium with E2 (39): they might seem to support the previous alternative suggestion (53–55) that these inhibitors drive the ATPase toward states which, at least in some respect, "differ" from the average E2 state prevailing at pH 6 in  $\text{Ca}^{2+}$ -free ATPase. In fact, in available crystals, the exact conformations of ATPase complexed with TG and CPA seem to be slightly different from each other (16, 17). However, old discussions in terms of "conformations" of enzymes during their catalytic cycle might be partly outdated by the more modern views about the intrinsic dynamics of protein structures, and our proteolysis data might be worth a comment in this respect. As an alternative to (or in addition to) the idea of TG shifting the "average" conformation of the protein into a slightly "different" one, we suggest that TG and the other inhibitors probably slow the cut at T242–E243 mainly because their "freezing" effect on the movements of the transmembrane segments of the ATPase propagates up to the links between the A-domain and the membrane domain: i.e., reduced susceptibility to proteolysis of the peripheral T242–E243 bond is probably not mainly due to steric hindrance in a new conformation, but to slowing of the protein dynamics in the region of these links, a slowing which turns out to be more or less similar for hydrophobic inhibitors bound at different sites near the transmembrane region. A similar slowing of the chain dynamics probably explains the protection of the cleavage sites around V734 and V747 in the M5 helix which is also observed upon TG binding (67). The ATPase might be inhibited as the result of such binding because protein "breathing" (i.e., transient increases in the protein transmembrane cross-sectional area) is probably involved in the various transitions in the catalytic cycle (24, 62). This could well be what has been dubbed by Logan-Smith et al. a "global conformational change" (64), except that we now might have to change our traditional loose way of talking about conformational changes into a more realistic one, taking into account the intrinsic flexibility and dynamic state of the protein.

The suggestion that the changes in proteolytic susceptibility of the T242–E243 bond observed in the present work after TG addition are due to changes in peptide chain dynamics, rather than to domain rotation and changes in bond

accessibility, makes even more remarkable the fact that the alternative explanation was correctly offered by Danko et al. (35) to explain the earlier and somewhat similar findings that the same T242–E243 bond was protected (but now fully) upon formation of E2P analogues (as confirmed in Figure 1): in that case, this alternative explanation did prove true, as rotation of the A-domain during the transition to E2P-related structures was subsequently deduced from crystal structures (10, 12).

To conclude, our main finding in this work is that, especially in the case of the formation of  $\text{Ca}^{2+}$ -free ATPase–fluoride complexes in the presence of beryllium, but also after the mere binding of ATP or  $\text{MgATP}$ , the membrane helices no longer respond to what is happening in the head domains after binding of TG or other inhibitors, as if the various regions of the protein were now "uncoupled". This is obviously due to the fact that the loops connecting the ATPase transmembrane and cytosolic domains are flexible. The role of these flexible links to accommodate thermal fluctuations and simultaneously permit coupling of  $\text{Ca}^{2+}$  transport to ATP hydrolysis has been discussed recently (17). Such flexibility might also be the basis for the long-disputed possible "slipping" of the pump under special circumstances (see, e.g., refs 63–65).

## ACKNOWLEDGMENT

We are grateful to David McIntosh for suggestions during this work and for his help in improving an initial version of the manuscript and to Hiroshi Suzuki for critical reading.

## SUPPORTING INFORMATION AVAILABLE

Figure S1 showing the protection of  $\text{E2}\cdot\text{MgF}_4$  and  $\text{E2}\cdot\text{VO}_4$  from proteolysis, in the absence or presence of TG; Figures S2–S4 showing FITC fluorescence changes upon addition of  $\text{VO}_4$  (or  $\text{AlF}_4$ ) and the effects of TG, BHQ, or CPA; Figure S5 showing Trp fluorescence responses to ATP (and  $[\gamma\text{-}^{32}\text{P}]\text{ATP}$  binding) in the presence of BHQ or CPA; Figure S6 showing the effect of DMSO and KCl on ATPase proteolysis; and Figure S7 showing that BHQ, too, favors p95 formation after proteolysis. This material is available free of charge via the Internet at <http://pubs.acs.org>.

## REFERENCES

- Makinose, M. (1972) Phosphoprotein formation during osmochemical energy conversion in the membrane of the sarcoplasmic reticulum, *FEBS Lett.* 25, 113–115.
- Hasselbach, W. (1978) The reversibility of the sarcoplasmic calcium pump, *Biochim. Biophys. Acta* 515, 23–53.
- de Meis, L., and Vianna, A. L. (1979) Energy interconversion by the  $\text{Ca}^{2+}$ -dependent ATPase of the sarcoplasmic reticulum, *Annu. Rev. Biochem.* 48, 275–292.
- Toyoshima, C., and Inesi, G. (2004) Structural basis of ion pumping by  $\text{Ca}^{2+}$ -ATPase of the sarcoplasmic reticulum, *Annu. Rev. Biochem.* 73, 269–292.
- Kühlbrandt, W. (2004) Biology, structure and mechanism of P-type ATPases, *Nat. Rev. Mol. Cell. Biol.* 5, 282–295.
- Møller, J. V., Nissen, P., Sørensen, T. L., and le Maire, M. (2005) Transport mechanism of the sarcoplasmic reticulum  $\text{Ca}^{2+}$ -ATPase pump, *Curr. Opin. Struct. Biol.* 15, 387–393.
- Toyoshima, C., Nakasako, M., Nomura, H., and Ogawa, H. (2000) Crystal structure of the calcium pump of sarcoplasmic reticulum at 2.6 Å resolution, *Nature* 405, 633–634.
- Toyoshima, C., and Nomura, H. (2002) Structural changes in the calcium pump accompanying the dissociation of calcium, *Nature* 418, 605–611.

9. Toyoshima, C., Nomura, H., and Sugita, Y. (2003) Structural basis of ion pumping by  $\text{Ca}^{2+}$ -ATPase of sarcoplasmic reticulum, *FEBS Lett.* 555, 106–110.
10. Sørensen, T. L.-M., Møller, J. V., and Nissen, P. (2004) Phosphoryl transfer and calcium ion occlusion in the calcium pump, *Science* 304, 1672–1675.
11. Toyoshima, C., and Mizutani, T. (2004) Crystal structure of the calcium pump with a bound ATP analogue, *Nature* 430, 529–535.
12. Toyoshima, C., Nomura, H., and Tsuda, T. (2004) Lumenal gating mechanism revealed in calcium pump crystal structures with phosphate analogues, *Nature* 442, 361–368.
13. Olesen, C., Sørensen, T. L.-M., Nielsen, R. C., Møller, J. V., and Nissen, P. (2004) Dephosphorylation of the calcium pump coupled to counterion occlusion, *Science* 306, 2251–2255.
14. Jensen, A.-M. L., Sørensen, T. L., Olesen, C., Møller, J. V., and Nissen, P. (2006) Modulatory and catalytic modes of ATP binding by the calcium pump, *EMBO J.* 25, 2305–2314.
15. Obara, K., Miyashita, N., Xu, C., Toyoshima, I., Sugita, Y., Inesi, G., and Toyoshima, C. (2005) Structural role of countertransport revealed in  $\text{Ca}^{2+}$  pump crystal structure in the absence of  $\text{Ca}^{2+}$ , *Proc. Natl. Acad. Sci. U.S.A.* 102, 14489–14496.
16. Moncoq, K., Trieber, C. A., and Young, H. S. (2007) The molecular basis for cyclopiazonic acid inhibition of the sarcoplasmic reticulum calcium pump, *J. Biol. Chem.* 282, 9748–9757.
17. Takahashi, M., Kondou, Y., and Toyoshima, C. (2007) Interdomain communication in calcium pump as revealed in the crystal structures with transmembrane inhibitors, *Proc. Natl. Acad. Sci. U.S.A.* 104, 5800–5805.
18. Toyoshima, C. (2007) Ion pumping by calcium ATPase of sarcoplasmic reticulum, *Adv. Exp. Med. Biol.* 592, 295–303.
19. Picard, M., Toyoshima, C., and Champeil, P. (2005) The average conformation at micromolar  $[\text{Ca}^{2+}]$  of  $\text{Ca}^{2+}$ -ATPase with bound nucleotide differs from that adopted with the transition state analog ADP·AlFx or with AMPPCP under crystallization conditions at millimolar  $[\text{Ca}^{2+}]$ , *J. Biol. Chem.* 280, 18745–18754.
20. Picard, M., Jensen, A.-M., Sørensen, T. L., Champeil, P., Møller, J. V., and Nissen, P. (2007)  $\text{Ca}^{2+}$  versus  $\text{Mg}^{2+}$  coordination at the nucleotide-binding site of the sarcoplasmic reticulum  $\text{Ca}^{2+}$ -ATPase, *J. Mol. Biol.* 368, 1–7.
21. Andersen, J. P., Møller, J. V., and Jørgensen, P. L. (1982) The functional unit of sarcoplasmic reticulum  $\text{Ca}^{2+}$ -ATPase. Active site titration and fluorescence measurements, *J. Biol. Chem.* 257, 8300–8307.
22. McIntosh, D. B., and Ross, D. C. (1985) Role of phospholipid and protein-protein associations in activation and stabilization of soluble  $\text{Ca}^{2+}$ -ATPase of sarcoplasmic reticulum, *Biochemistry* 24, 1244–1251.
23. Lund, S., Orlowski, S., de Foresta, B., Champeil, P., le Maire, M., and Møller, J. V. (1989) Detergent structure and associated lipid as determinants in the stabilization of solubilized  $\text{Ca}^{2+}$ -ATPase from sarcoplasmic reticulum, *J. Biol. Chem.* 264, 4907–4915.
24. Picard, M., Dahmane, T., Garrigos, M., Gauron, C., Giusti, F., le Maire, M., Popot, J.-L., and Champeil, P. (2006) Protective and inhibitory effects of various types of amphipols on the  $\text{Ca}^{2+}$ -ATPase from sarcoplasmic reticulum: a comparative study, *Biochemistry* 45, 1861–1869.
25. Sagara, Y., Wade, J. B., and Inesi, G. (1992) A conformational mechanism for formation of a dead-end complex by the sarcoplasmic reticulum ATPase with thapsigargin, *J. Biol. Chem.* 267, 1286–1292.
26. Wictome, M., Michelangeli, F., Lee, A. G., and East, J. M. (1992) The inhibitors thapsigargin and 2,5-di(tert-butyl)-1,4-benzohydroquinone favour the E2 form of the  $\text{Ca}^{2+}$ ,  $\text{Mg}^{2+}$ -ATPase, *FEBS Lett.* 304, 109–113.
27. Seekoe, T., Peall, S., and McIntosh, D. B. (2001) Thapsigargin and dimethyl sulfoxide activate Medium Pi  $\leftrightarrow$  HOH oxygen exchange catalyzed by sarcoplasmic reticulum  $\text{Ca}^{2+}$ -ATPase, *J. Biol. Chem.* 276, 46737–46744.
28. Picard, M., Toyoshima, C., and Champeil, P. (2006) Effects of inhibitors on luminal opening of  $\text{Ca}^{2+}$  binding sites in an E2P-like complex of sarcoplasmic reticulum  $\text{Ca}^{2+}$ -ATPase with  $\text{Be}^{2+}$ -fluoride, *J. Biol. Chem.* 281, 3360–3369.
29. Champeil, P., Guillain, F., Vénien, C., and Gingold, M. P. (1985) Interaction of magnesium and inorganic phosphate with calcium-depleted sarcoplasmic reticulum adenosinetriphosphatase as reflected by organic solvent induced perturbation, *Biochemistry* 24, 69–81.
30. Juul, B., Turc, H., Durand, M. L., Gomez de Gracia, A., Denoroy, L., Møller, J. V., Champeil, P., and le Maire, M. (1995) Do transmembrane segments in proteolyzed sarcoplasmic reticulum  $\text{Ca}^{2+}$ -ATPase retain their functional  $\text{Ca}^{2+}$  binding properties after removal of cytoplasmic fragments by proteinase K?, *J. Biol. Chem.* 270, 20123–20134.
31. Møller, J. V., Lenoir, G., Marchand, C., Montigny, C., le Maire, M., Toyoshima, C., Juul, B. S., and Champeil, P. (2002) Calcium transport by sarcoplasmic reticulum  $\text{Ca}^{2+}$ -ATPase. Role of the A-domain and its C-terminal link with the transmembrane region, *J. Biol. Chem.* 277, 38647–38659.
32. Soulié, S., Møller, J. V., Falson, P., and le Maire, M. (1996) Urea reduces the aggregation of membrane proteins on Sodium Dodecyl Sulfate-Polyacrylamide Gel Electrophoresis, *Anal. Biochem.* 236, 363–364.
33. Laemmli, U. K. (1970) Cleavage of structural proteins during the assembly of the head of bacteriophage T4, *Nature* 227, 680–685.
34. Champeil, P., Riollot, S., Orlowski, S., Guillain, F., Seebregts, C. J., and McIntosh, D. B. (1988) ATP regulation of sarcoplasmic reticulum  $\text{Ca}^{2+}$ -ATPase. Metal-free ATP and 8-bromo-ATP bind with high affinity to the catalytic site of phosphorylated ATPase and accelerate dephosphorylation, *J. Biol. Chem.* 263, 12288–12294.
35. Danko, S., Daiho, T., Yamasaki, K., Kamidochi, M., Suzuki, H., and Toyoshima, C. (2001) ADP-insensitive phosphoenzyme intermediate of sarcoplasmic reticulum  $\text{Ca}^{2+}$ -ATPase has a compact conformation resistant to proteinase K, V8 protease and trypsin, *FEBS Lett.* 489, 277–282.
36. Danko, S., Yamasaki, K., Daiho, T., and Suzuki, H. (2004) Distinct natures of Beryllium Fluoride-bound, Aluminum Fluoride-bound, and Magnesium Fluoride-bound stable analogues of an ADP-insensitive Phosphoenzyme intermediate of sarcoplasmic reticulum  $\text{Ca}^{2+}$ -ATPase: changes in catalytic and transport sites during phosphoenzyme hydrolysis, *J. Biol. Chem.* 279, 14991–14998.
37. de Meis, L., Martins, O. B., and Alves, E. W. (1980) Role of water, Hydrogen ion, and temperature on the synthesis of ATP by the sarcoplasmic reticulum adenosinephosphatase as reflected by organic solvent induced perturbation, *Biochemistry* 19, 4252–4261.
38. Sagara, Y., Fernandez-Belda, F., de Meis, L., and Inesi, G. (1992) Characterization of the inhibition of intracellular  $\text{Ca}^{2+}$  transport ATPases by thapsigargin, *J. Biol. Chem.* 267, 12606–12613.
39. Pick, U., and Karlisch, S. J. (1982) Regulation of the conformation transition in the Ca-ATPase from sarcoplasmic reticulum by pH, temperature, and calcium ions, *J. Biol. Chem.* 257, 6120–6126.
40. Kijima, Y., Ogunbunmi, E., and Fleischer, S. (1991) Drug action of thapsigargin on the  $\text{Ca}^{2+}$  pump protein of sarcoplasmic reticulum, *J. Biol. Chem.* 266, 22912–22918.
41. McIntosh, D. B., Woolley, D. G., Vilsen, B., and Andersen, J. P. (1996) Mutagenesis of Segment 487Phe-Ser-Arg-Asp-Arg-Lys492 of sarcoplasmic reticulum  $\text{Ca}^{2+}$ -ATPase produces pumps defective in ATP binding, *J. Biol. Chem.* 271, 25778–25789.
42. McIntosh, D. B., Woolley, D. G., MacLennan, D. H., Vilsen, B., and Andersen, J. P. (1999) Interaction of nucleotides with Asp351 and the conserved phosphorylation loop of sarcoplasmic reticulum  $\text{Ca}^{2+}$ -ATPase, *J. Biol. Chem.* 274, 25227–25236.
43. Guillain, F., Gingold, M. P., and Champeil, P. (1982) Direct fluorescence measurements of  $\text{Mg}^{2+}$  binding to sarcoplasmic reticulum ATPase, *J. Biol. Chem.* 257, 7366–7371.
44. Dupont, Y., Bennett, N., and Lacapère, J.-J. (1982) Fluorescence studies of the sarcoplasmic reticulum calcium pump, *Ann. N. Y. Acad. Sci.* 402, 569–572.
45. Lacapère, J.-J., Bennett, N., Dupont, Y., and Guillain, F. (1990) pH and magnesium dependence of ATP binding to sarcoplasmic reticulum ATPase. Evidence that the catalytic ATP-binding site consists of two domains, *J. Biol. Chem.* 265, 345–353.
46. DeJesus, F., Girardet, J. L., Dupont, Y. (1993) Characterisation of ATP binding inhibition to the sarcoplasmic reticulum  $\text{Ca}^{2+}$ -ATPase by thapsigargin, *FEBS Lett.* 332, 229–232.
47. Clausen, J. D., McIntosh, D. B., Anthonisen, A. N., Woolley, D. G., Vilsen, B., and Andersen, J. P. (2007) ATP-binding modes and functionally important interdomain bonds of sarcoplasmic reticulum  $\text{Ca}^{2+}$ -ATPase revealed by mutation of Glycine 438, Glutamate 439, and Arginine 678, *J. Biol. Chem.* (in press).

48. Champeil, P., Menguy, T., Soulié, S., Juul, B., Gomez, de Gracia, A., Rusconi, F., Falson, P., Denoroy, L., Henao, F., le Maire, M., and Møller, J. V. (1998) Characterization of a protease-resistant domain of the cytosolic portion of sarcoplasmic reticulum  $\text{Ca}^{2+}$ -ATPase. Nucleotide and metal binding sites, *J. Biol. Chem.* 273, 6619–6631.
49. Lenoir, G., Picard, M., Gauron, C., Montigny, C., Le, Maréchal, P., Falson, P., le Maire, M., Møller, J. V., and Champeil, P. (2004) Functional properties of sarcoplasmic reticulum  $\text{Ca}^{2+}$ -ATPase after proteolytic cleavage at Leu119-Lys120, close to the A-domain, *J. Biol. Chem.* 279, 9156–9166.
50. Xu, C., Ma, H., Inesi, G., Al-Shawi, M. K., and Toyoshima, C. (2004) Specific structural requirements for the inhibitory effect of Thapsigargin on the  $\text{Ca}^{2+}$  ATPase SERCA, *J. Biol. Chem.* 279, 17973–17979.
51. Sagara, Y., and Inesi, G. (1991) Inhibition of the sarcoplasmic reticulum  $\text{Ca}^{2+}$  transport ATPase by thapsigargin at subnanomolar concentrations, *J. Biol. Chem.* 266, 13503–13506.
52. Forge, V., Mintz, E., and Guillain, F. (1993)  $\text{Ca}^{2+}$  binding to sarcoplasmic reticulum ATPase revisited. I. Mechanism of affinity and cooperativity modulation by  $\text{H}^{+}$  and  $\text{Mg}^{2+}$ , *J. Biol. Chem.* 268, 10953–10968.
53. Wictome, M., Khan, Y. M., Lee, A. G., and East, J. M. (1995) Binding of sesquiterpene lactone inhibitors to the  $\text{Ca}^{2+}$ -ATPase, *Biochem. J.* 310, 859–868.
54. Khan, Y. M., Wictome, M., East, J. M., and Lee, A. G. (1995) Interactions of dihydroxybenzenes with the  $\text{Ca}^{2+}$ -ATPase: separate binding sites for dihydroxybenzenes and sesquiterpene lactones, *Biochemistry* 34, 14385–14393.
55. Logan-Smith, M. J., East, J. M., and Lee, A. G. (2002) Evidence for a global inhibitor-induced conformation change on the  $\text{Ca}^{2+}$ -ATPase of sarcoplasmic reticulum from paired inhibitor studies, *Biochemistry* 41, 2869–2875.
56. Ma, H., Zhong, L., Inesi, G., Fortea, I., Soler, F., and Fernandez-Belda, F. (1999) Overlapping effects of S3 stalk segment mutations on the affinity of  $\text{Ca}^{2+}$ -ATPase (SERCA) for thapsigargin and cyclopiazonic acid, *Biochemistry* 38, 15522–15527.
57. Champeil, P., Gingold, M. P., Guillain, F., and Inesi, G. (1983) Effect of magnesium on the calcium-dependent transient kinetics of sarcoplasmic reticulum ATPase, studied by stopped flow fluorescence and phosphorylation, *J. Biol. Chem.* 258, 4453–4458.
58. Lenoir, G., Jaxel, C., Picard, M., le Maire, M., Champeil, P., and Falson, P. (2006) Conformational changes in sarcoplasmic reticulum  $\text{Ca}^{2+}$ -ATPase mutants: effect of mutations either at  $\text{Ca}^{2+}$ -binding Site II or at tryptophan 552 in the cytosolic domain, *Biochemistry* 45, 5261–5270.
59. McIntosh, D. B., Clausen, J. C., Woolley, D. G., MacLennan, D. H., Vilsen, B., and Andersen, J. P. (2004) Roles of conserved P-domain residues and  $\text{Mg}^{2+}$  in ATP binding in the ground and  $\text{Ca}^{2+}$ -activated states of sarcoplasmic reticulum  $\text{Ca}^{2+}$ -ATPase, *J. Biol. Chem.* 279, 32515–32523.
60. Davidson, G., and Varhol, R. J. (1995) Kinetics of thapsigargin- $\text{Ca}^{2+}$ -ATPase (sarcoplasmic reticulum) interaction reveals a two-step binding mechanism and picomolar inhibition, *J. Biol. Chem.* 270, 11731–11734.
61. Champeil, P., le Maire, M., Møller, J. V., Riollot, S., Guillain, F., and Green, N. M. (1986) Does intrinsic fluorescence reflect conformational changes in the  $\text{Ca}^{2+}$ -ATPase of sarcoplasmic reticulum?, *FEBS Lett.* 206, 93–98.
62. Cantor, R. S. (1997) The lateral pressure profile in membrane: A physical mechanism of general anesthesia, *Biochemistry* 36, 2339–2344.
63. de Meis, L. (2001) Uncoupled ATPase activity and heat production by the sarcoplasmic reticulum  $\text{Ca}^{2+}$ -ATPase. Regulation by ADP, *J. Biol. Chem.* 276, 25078–25087.
64. Logan-Smith, M. J., Lockyer, P. J., East, J. M., and Lee, A. G. (2001) Curcumin, a molecule that inhibits the  $\text{Ca}^{2+}$ -ATPase of sarcoplasmic reticulum but increases the rate of accumulation of  $\text{Ca}^{2+}$ , *J. Biol. Chem.* 276, 46905–46911.
65. Sumbilla, C., Lewis, D., Hammerschmidt, T., and Inesi, G. (2002) The slippage of the  $\text{Ca}^{2+}$  pump and its control by anions and curcumin in skeletal and cardiac sarcoplasmic reticulum, *J. Biol. Chem.* 277, 13900–13906.
66. Champeil, P., Henao, F., Lacapère, J.-J., and McIntosh, D. B. (2001) A remarkably stable phosphorylated form of  $\text{Ca}^{2+}$ -ATPase prepared from  $\text{Ca}^{2+}$ -loaded and fluorescein isothiocyanate-labeled sarcoplasmic reticulum vesicles, *J. Biol. Chem.* 276, 5795–5803.
67. Inesi, G., Lewis, D., Ma, H., Prasad, A., and Toyoshima, C. (2006) Concerted conformational effects of  $\text{Ca}^{2+}$  and ATP are required for activation of sequential reactions in the  $\text{Ca}^{2+}$  ATPase (SERCA) catalytic cycle, *Biochemistry* 45, 13769–13778.

BI701855R